Published online: October 27, 2015

Article

SOURCE DATA | TRANSPARENT PROCESS

EMBO reports

Ubiquitin-Activated Interaction Traps (UBAITs) identify E3 ligase binding partners

Hazel F O'Connor, Nancy Lyon, Justin W Leung, Poonam Agarwal, Caleb D Swaim, Kyle M Miller & Jon M Huibregtse*

Abstract

We describe a new class of reagents for identifying substrates, adaptors, and regulators of HECT and RING E3s. UBAITs (Ubiquitin-Activated Interaction Traps) are E3-ubiquitin fusion proteins and, in an E1- and E2-dependent manner, the C-terminal ubiquitin moiety forms an amide linkage to proteins that interact with the E3, enabling covalent co-purification of the E3 with partner proteins. We designed UBAITs for both HECT (Rsp5, Itch) and RING (Psh1, RNF126, RNF168) E3s. For HECT E3s, trapping of interacting proteins occurred *in vitro* either through an E3 thioester-linked lariat intermediate or through an E2 thioester intermediate, and both WT and active-site mutant UBAITs trapped known interacting proteins in yeast and human cells. Yeast Psh1 and human RNF126 and RNF168 UBAITs also trapped known interacting proteins when expressed in cells. Human RNF168 is a key mediator of ubiquitin signaling that promotes DNA double-strand break repair. Using the RNF168 UBAIT, we identify H2AZ—a histone protein involved in DNA repair—as a new target of this E3 ligase. These results demonstrate that UBAITs represent powerful tools for profiling a wide range of ubiquitin ligases.

Keywords HECT E3s; RING E3s; Ubiquitin; Ubiquitin ligases
Subject Categories Methods & Resources; Post-translational Modifications, Proteolysis & Proteomics
DOI 10.15252/embr.201540620 | Received 30 April 2015 | Revised 26 August 2015 | Accepted 28 August 2015 | Published online 27 October 2015
EMBO Reports (2015) 16: 1699–1712

Introduction

Ubiquitin is a post-translational modifier that determines the fate of a large fraction of all proteins in eukaryotic cells, and the specificity of ubiquitylation is controlled by hundreds of ubiquitin ligases (> 600 in human cells) [1]. The complex network of enzyme–substrate interactions that mediate ubiquitylation is only partially characterized, with the vast majority of E3s remaining essentially uncharacterized with respect to substrates and functions. Unraveling this network has the potential to yield many insights into cellular regulation and disease pathways and provide innumerable opportunities for developing clinically useful modulators of specific E3s or classes of E3s [2].

E3 enzymes interact either directly or indirectly, via adaptor proteins, with their substrates. In human cells, E3s are supported by two E1 enzymes (Uba1 and Uba6) and approximately 60 E2 enzymes [3,4]. The E1 enzymes activate ubiquitin in an ATP-dependent reaction and transfer ubiquitin to E2 proteins, catalyzing formation of a thioester bond between the terminal carboxyl group of ubiquitin and the active-site cysteine of the E2s [5]. RING E3s are the most numerous type of ubiquitin ligases, representing approximately 95% of all E3s encoded by human cells [1]. The RING domain forms a platform for recruiting a ubiquitin-charged E2 protein. The E3 facilitates transfer of ubiquitin from the E2 to one or more lysines of an E3-bound substrate [6,7] and can activate the E2 for discharge of ubiquitin [8–11]. For simple RING E3s, substrate recruitment is mediated by other domains within the E3 protein, while for more complex E3s, such as CRLs, other proteins within the multi-protein complex mediate substrate recognition (e.g., F-box proteins). RING E3s control a wide range of cellular processes and play a key role in a wide range of human disease states, including cancer and the innate immune response to viral infections (Mdm2 and TRIM5, respectively) [12,13].

HECT E3s are relatively few in number, with five in *Saccharomyces cerevisiae* and 28 human HECT E3s. They are defined by a approximately 350 amino acid C-terminal catalytic domain (the HECT domain) and range in size from approximately 90 kDa to over 500 kDa. The regions N-terminal to the HECT domain are involved in substrate recognition, localization, and regulation [14]. Structures of isolated HECT domains have revealed that the catalytic domain consists of an approximately 250 amino acid N-terminal lobe, containing the E2 binding site, and a approximately 100 amino acid C-terminal lobe, containing the active-site cysteine [15–17]. The HECT domain binds ubiquitin-charged E2s, ubiquitin is transferred to the active-site cysteine of the E3, and the E3 directly catalyzes substrate ubiquitylation.

In some cases, substrate recognition by HECT E3s is mediated by obvious protein–protein interaction modules, such as WW domains. WW domains define the Nedd4 subfamily of HECT E3s, which includes *S. cerevisiae* Rsp5 and human Nedd4, Nedd4L, Itch, and others [18]. WW domains are 30–45 amino acids in length and recognize proline-containing "PY" motifs (PPXY consensus), with most Nedd4 family substrates, substrate adaptors, or regulatory

Department of Molecular Biosciences and Institute for Cellular and Molecular Biology, University of Texas at Austin, Austin, TX, USA
*Corresponding author. Tel: +1 512 232 7700; E-mail: huibregtse@austin.utexas.edu

Published online: October 27, 2015
EMBO reports

proteins containing one or more PY motifs [19–22]. At least half of all human HECT E3s do not have obvious protein–protein interaction modules, and a basis for substrate recognition is not readily apparent. Such an example is human E6AP/Ube3A, which is involved in HPV-associated cervical cancer and Angelman syndrome, a severe neurologic disease [23–25]. Other HECT E3s involved in important aspects of human biology include Huwe1/Arf-BP1, Herc1, Herc2, and Herc5 [26]. A third class of E3s, the RBR E3s, have biochemical characteristics of both RING and HECT E3s, in that they contain a RING domain that recruits an E2 enzyme, yet they also contain an active-site cysteine that accepts ubiquitin from the E2 and transfers it to substrate proteins [27–29]. Important members of this class of E3s include Parkin, HOIP, and HHARI [30].

Many genetic and biochemical approaches have been employed to identify substrates and regulatory proteins of E3s, including yeast two-hybrid assays, co-immunoprecipitation approaches, and protein–protein interaction arrays [31–35]. While each of these has its own advantages and disadvantages, we sought a method that would be applicable to a wide range of E3s and would overcome the challenges posed by potentially weak or transient enzyme–substrate interactions. We describe a method, based on E3-ubiquitin fusion proteins, to covalently trap E3s to their substrates and other interacting proteins.

Results

HECT E3 UBAITs

The C-terminus of ubiquitin is critical for all chemistry involved in ubiquitin activation and conjugation. Ubiquitin molecules with small N-terminal epitopes are generally very good substrates in conjugation reactions (e.g., 6×His-Ub [36]), and we envisioned that a very large N-terminal epitope—consisting of a approximately 100-kDa HECT E3 with a flexible linker connecting it to ubiquitin—might also be competent for activation by the E1 ubiquitin-activating enzyme and subsequent transfer to an E2 enzyme (Fig 1A; species i and ii, respectively). If so, we predicted, based on the structure of a HECT domain in complex with an E2~ubiquitin complex [37], that the active-site thiolate of the HECT domain might be able to attack the Ub~E2 thioester bond in an intramolecular reaction, forming a thioester-linked protein lariat (Fig 1A, species iii). The reaction of a substrate lysine with the lariat protein would then yield an amide-linked E3-Ub-target protein complex (Fig 1A, species v), thus covalently "trapping" the substrate protein to its E3. Alternatively, even if the lariat structure did not form, the direct reaction of a substrate lysine with the Ub~E2 thioester would be predicted to yield an identical product (species v, via species iv). In both cases, affinity purification of the HECT-Ub fusion protein would co-purify covalently trapped target proteins, which could then be identified by standard LC-MS/MS techniques. We refer to these tools for identification of substrates, and potentially regulatory or other interacting proteins, as UBAITs, for Ubiquitin-Activated Interaction Traps.

Characterization of Rsp5 UBAITs *in vitro*

Saccharomyces cerevisiae Rsp5 is one of the most extensively characterized HECT E3s, with many identified substrates, adaptors, and

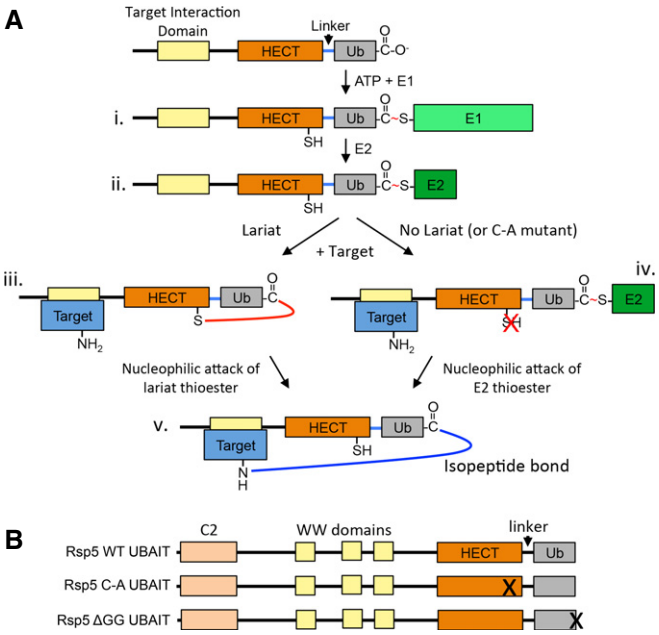

Figure 1. The UBAIT concept.

A Schematic of proposed UBAIT mechanism. The E1 enzyme activates the UBAIT, forming a thioester-linked complex (i.), which is then transferred to an E2 enzyme (ii.). The active-site cysteine of the E3 can attack the E2 thioester, forming a thioester-linked protein lariat structure (iii.); when an amine group of a target protein attacks the thioester bond, a stable amide linkage is formed between the UBAIT and the target protein (v.). If the UBAIT does not form a lariat structure, as in the case of the active-site mutant (iv.), an amine group of a target protein can potentially directly attack the E2 thioester bond, also resulting in a covalent UBAIT-target protein complex (v.).

B Depiction of the wild-type Rsp5 UBAIT (WT), active-site cysteine mutant (C-A) UBAIT, and ΔGG ubiquitin (ΔGG) UBAIT.

regulatory proteins [38,39]. We purified bacterially expressed Rsp5 UBAITs with a 12-amino acid linker (consisting of GA dipeptide repeat) between the E3 and ubiquitin (Fig 1B). UBAITs consisted of either wild-type Rsp5 fused to wild-type ubiquitin (WT UBAIT), the Rsp5 active-site C-to-A mutant fused to wild-type ubiquitin (C-A UBAIT), or wild-type Rsp5 fused to a non-conjugatable form of ubiquitin (ΔGG UBAIT, deleted of the terminal GG residues). The UBAITs were ^{32}P-labeled at an N-terminal kinase recognition epitope and assayed for their ability to form E1 and E2 thioester complexes. As shown in Fig 2A, the WT UBAIT formed an E1 thioester in the presence of E1 alone (lane 2), and the addition of both E1 and E2 (lane 4), but not E2 alone (lane 3), resulted in the appearance of a band of the predicted size for a UBAIT~E2 adduct. The E1 and E2 adducts were greatly diminished in the presence of DTT (lanes 6 and 8), although residual E2 adducts remained (lane 8), likely a reflection of E2 auto-conjugation (i.e., auto-UBAITylation). These results indicate that the ubiquitin moiety of the wild-type Rsp5 UBAIT is competent for activation by E1 and transfer to E2. The Rsp5 C-A UBAIT behaved identically to the WT UBAIT in the E1 and E2 thioester assays, while the ΔGG UBAIT, as expected, did not form any E1 or E2 adducts (H.F. O'Connor and J.M. Huibregtse, unpublished observation). No extra bands with the WT UBAIT, corresponding to a potential lariat thioester, were detected in the

Published online: October 27, 2015

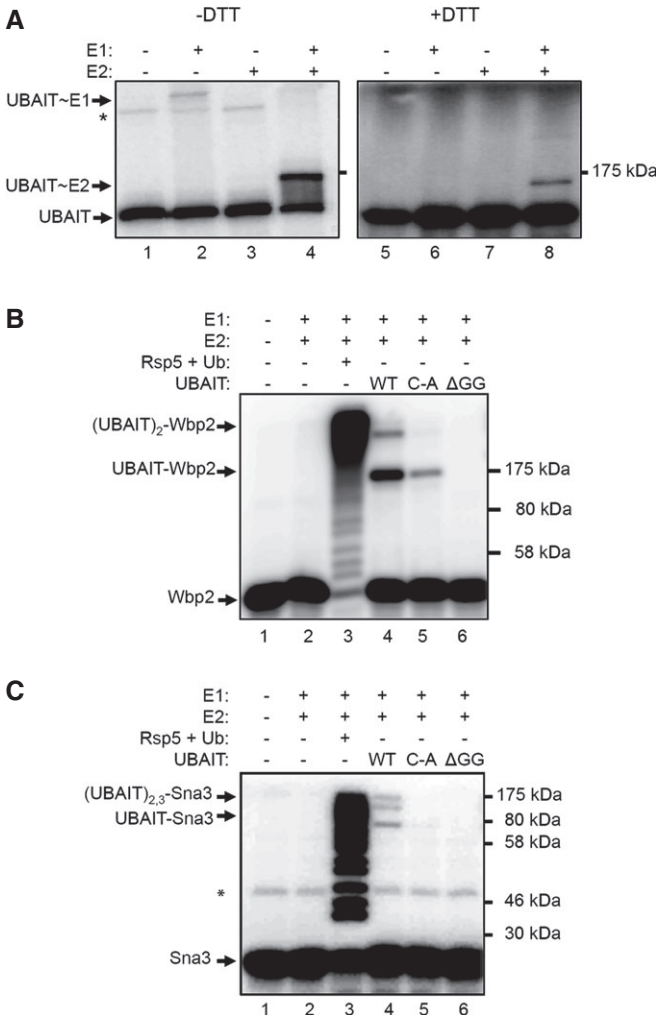

Figure 2. Rsp5 UBAITs are functional *in vitro*.

A Rsp5 can be activated by E1 and transferred to an E2. Purified ^{32}P-labeled Rsp5 UBAIT (WT) was incubated with or without E1 and E2 enzymes, and products were analyzed by SDS–PAGE in the absence or presence of DTT in the loading buffer. The migration points of the UBAIT~E1 and UBAIT~E2 thioesters are indicated. The asterisk marks a contaminant of the purification process (uncut GST-tagged UBAIT).

B Rsp5 UBAITs were incubated with E1 and E2 proteins, as indicated, and ^{32}P-labeled Wbp2. The migration points of the major products are indicated with arrows.

C Rsp5 UBAITs were incubated with E1 and E2 proteins, as indicated, and ^{32}P-labeled Sna3. The migration points of the major products are indicated with arrows. The asterisk marks a contaminant of the purification process (uncut GST-Sna3).

presence of E1 and E2, although the lariat would not necessarily migrate differently than the UBAIT protein, itself.

To determine whether the Rsp5 UBAIT was capable of covalently trapping targets *in vitro*, the WT, C-A, and ΔGG UBAITs were combined with E1 and E2 proteins and a ^{32}P-labeled target protein, either human Wbp2 or yeast Sna3 K125 (a single-lysine derivative of Sna3). Both Wbp2 and Sna3 contain PY motifs and interact with the WW domains of Rsp5 [40]. As expected, Rsp5 (with no ubiquitin fusion) efficiently ubiquitylated both substrates in the presence of free ubiquitin (lane 3 of Fig 2B and C), while the WT UBAIT, but not the ΔGG, formed a stable covalent conjugate of the predicted size to both target proteins (compare lanes 4 and 6 of Fig 2B and C). Conjugate formation with the WT UBAIT was shown to be dependent on the PY motif of Sna3 (Appendix Fig S1). Higher molecular weight conjugates corresponded in size to multi-UBAITylated targets, which are likely to arise due to binding of the PY motif of a UBAIT-target conjugate to a WW domain of a second UBAIT molecule. The apparent inefficiency of the substrate UBAITylation reaction compared to the substrate ubiquitylation catalyzed by Rsp5 is due, at least in part, to the fact that the UBAIT reaction is single-turnover, whereas Rsp5 rapidly depletes free substrate by polyubiquitylating many molecules of the substrate over a relatively short time period [40]. Interestingly, the C-A mutant UBAIT also formed conjugates to both target proteins (lane 5, Fig 2B and C), although less efficiently than with WT UBAIT, particularly for Sna3. This suggests that the Rsp5 UBAIT is capable of trapping targets by both mechanisms illustrated in Fig 1A: either through nucleophilic attack of an E3-Ub lariat intermediate, or by direct attack of the E2 thioester. Based on the relative efficiency of the WT UBAIT to C-A UBAIT reactions, the lariat mechanism appears to be the predominate mechanism *in vitro*.

We examined the effect of the linker length on target trapping *in vitro* by expressing Rsp5 UBAITs containing a GGSG flexible linker sequence [33,41,42] repeated 1, 3, or 5 times, resulting in linker lengths of 4, 12, or 20 amino acids. As shown in Appendix Fig S2, all three WT UBAITs supported target trapping *in vitro*, with the longer linker lengths supporting more efficient conjugation to Wbp2. Therefore, a range of linker lengths appears to be permissible for the Rsp5 UBAIT, with a longer linker being generally more favorable.

In vivo validation of Rsp5 UBAITs

To determine whether UBAITs were able to trap substrates or interacting proteins *in vivo*, N-terminal TAP-tagged Rsp5 UBAITs (WT, C-A, and ΔGG, with a 12-amino acid GA-repeat linker) and a TAP-only control protein (consisting of two copies of protein A and the calmodulin-binding protein) were expressed from a galactose-regulated multicopy plasmid in a wild-type *RSP5* haploid yeast strain. An anti-TAP immunoblot showed a similar distribution of high molecular weight conjugates for both the WT and C-A UBAITs (Appendix Fig S3), suggesting that the non-lariat mechanism of UBAITylation may predominate *in vivo*. The ΔGG UBAIT showed no apparent conjugates, as expected. Appendix Fig S4A shows that TAP-tagged Rsp5 (non-UBAIT) was expressed similarly to the WT and ΔGG UBAITs, indicating that the ubiquitin moiety did not result in destabilization of the UBAITs. In addition, the Rsp5 UBAITs were expressed at a similar level to the endogenous Rsp5 protein (H.F. O'Connor, N. Lyon and J.M. Huibregtse, unpublished observation), as reported previously for expression of other Rsp5 variants expressed from the same plasmid [43].

To identify the Rsp5 UBAIT conjugates, expression of the TAP-UBAIT proteins was induced for three hours, cell lysates were prepared, and the proteins were affinity-purified via the protein A tag on IgG sepharose. Bound proteins were then denatured with SDS and heat and, after dilution of the SDS, purified on IgG sepharose a second time. The final products were subjected to SDS–PAGE, and gel slices were excised from above the migration point of the TAP-Rsp5 proteins (approximately 130 kDa). In-gel tryptic digestions

were performed, and peptides were identified by LC-MS/MS. Results were analyzed using Thermo Proteome Discoverer software with high stringency filters. Proteins with two or more spectral counts from the WT UBAIT sample and greater than or equal to five-fold higher spectral counts in the WT UBAIT sample compared to the TAP control were considered "positive hits" and potential Rsp5-interacting proteins. Table 1 shows the total spectral counts for known Rsp5-interacting proteins that met the filtering criteria in two biological replicates (25 total proteins), and Appendix Table S1 shows an additional 57 proteins that also met filtering criteria and have not previously been reported to interact with Rsp5. Among the known Rsp5-interacting proteins were regulatory proteins (Rup1, Ubp2), substrates (Mup1, Zrt1, Sec7, Rpb1, Mga2), and adaptor proteins (Art5, Rvs167, Lsb1, Bsd2) (Table 1). The potential novel interactors included Sul2 (a sulfur permease), two plasma membrane-associated t-SNAREs (Sso1 and Sso2), and Rvs161, a lipid raft protein that interacts with Rvs167 [44], a known Rsp5 target protein (Appendix Table S1).

Further examination of the Rsp5-interacting proteins showed that they fell into two groups with respect to UBAIT trapping. The first group contained proteins that were isolated with both the WT and C-A UBAITs, but not the ΔGG UBAIT. There were no proteins that were isolated solely with the WT UBAIT, further indicating that the predominant mechanism of trapping *in vivo* was the non-lariat mechanism. Both known and potentially novel Rsp5 interacting proteins were present in this group, as well as a subset of ubiquitin E2 proteins (Ubc4, Ubc6, and Ubc13), which were likely to have been isolated as a result of E2 auto-UBAITylation (as observed *in vitro*; Fig 2A). The second group of proteins was, surprisingly, isolated with all three UBAITs, including the non-conjugatable ΔGG UBAITs, suggesting that these were isolated via non-covalent binding to the Rsp5 proteins. Many of these proteins were well-characterized Rsp5-interacting proteins, including Bul1, several Art proteins (Art1, Art3, Art4, Art6, Art8), and Rpb1 [32,45–48]. In general, the spectral counts for these conjugation-independent hits were among the highest of any of the proteins identified, consistent

Table 1. Known Rsp5-interacting proteins isolated with Rsp5 UBAITs in *Saccharomyces cerevisae*.

			Experiment 1				Experiment 2				
ACC#	Protein	MW [kDa]	WT	C-A	ΔGG	TAP	WT	C-A	ΔGG	TAP	PY-like motif
Q12502	ART1	89.8	64	70	23	0	19	40	38	0	no
P47029	ART3	117.1	153	206	113	0	92	110	78	0	no
Q02805	ART4	92.3	76	45	50	0	26	18	12	0	yes
P53244	ART5	65.4	56	41	0	0	14	14	0	0	yes
P36117	ART6	102.5	169	215	147	0	59	80	69	0	yes
Q12734	ART8	124.8	181	135	155	0	45	55	98	0	yes
P38356	BSD2	35.7	5	13	0	0	2	5	0	0	yes
P48524	BUL1	109.1	67	89	142	0	47	64	98	0	yes
P54005	DIA1	38.7	8	15	0	0	3	8	0	0	yes
Q03212	EAR1	62.5	5	24	1	0	2	13	2	0	yes
P53281	LSB1	26.1	124	85	3	0	77	80	13	0	yes
P40578	MGA2	127.0	2	2	3	0	2	3	2	0	yes
P50276	MUP1	63.2	3	6	0	0	6	11	0	0	no
Q06449	PIN3	23.5	49	45	0	0	33	39	7	0	yes
P38212	RCR1	23.9	26	30	0	0	11	21	0	0	yes
P04050	RPB1	191.5	5,490	4,191	9,127	186	2,335	1,726	2,201	287	yes
Q12242	RUP1	75.3	28	13	2	0	15	3	0	0	yes
P39743	RVS167	52.7	208	253	0	0	73	91	0	0	yes
P11075	SEC7	226.7	15	5	0	0	6	0	1	0	yes
P14359	SNA3	15.2	40	30	0	0	36	22	3	1	yes
P32343	SSH4	65.0	34	45	6	0	9	23	12	0	yes
P15731	UBC4	16.4	10	11	0	0	14	16	0	0	yes
Q01476	UBP2	146.3	135	37	1	1	67	16	14	3	yes
P54787	VPS9	52.4	2	1	0	0	6	1	0	0	yes
P32804	ZRT1	41.6	53	89	0	0	20	37	8	0	yes

Total spectral counts of known Rsp5-interacting proteins isolated with the Rsp5 WT UBAIT, C-A UBAIT, ΔGG UBAIT, and empty TAP control (TAP). Proteins shown passed the following filtering criteria in two biological replicates (Experiments 1 and 2): two or more spectral counts for the WT sample and greater than or equal to five-fold more counts in WT sample compared to TAP control. Identified proteins were analyzed for the presence of PY-like motifs [94].

with these proteins being among the most abundant and/or robust Rsp5-interacting proteins. It is likely that these proteins were able to re-bind non-covalently to the Rsp5 proteins in the second IgG pull-down, after denaturation and subsequent dilution of the SDS. To test this possibility, an additional experiment was performed with the WT and ΔGG UBAITs in parallel with TAP-Rsp5 (non-UBAIT) as a control. As shown in Appendix Table S2, the same proteins that were isolated with the ΔGG UBAIT were also isolated with Rsp5 (non-UBAIT). In contrast, those that had only been isolated with the WT and C-A UBAITs (and not the ΔGG UBAIT) were not isolated with TAP-Rsp5 (Appendix Table S3). As most of these non-covalently interacting proteins were *bona fide* Rsp5-interacting proteins, further attempts to eliminate them during purification were not made.

A potential caveat to the UBAIT approach is the use of the UBAIT as a source of ubiquitin in reactions catalyzed by other cellular E3s. We therefore determined whether Rsp5 (non-UBAIT) could utilize, *in vitro*, a RING E3 UBAIT (based on Psh1; discussed further below) as the source of ubiquitin in a ubiquitylation reaction. As shown in Appendix Fig S5, Rsp5 could indeed use Psh1-Ub as a source of ubiquitin to modify Wbp2 *in vitro*. This suggests that many other cellular E3s might also be capable of using a large ubiquitin fusion protein in a substrate ubiquitylation reaction. At one extreme, one might therefore have expected to isolate the complete cellular "ubiquitinome" with the Rsp5 UBAIT. This clearly was not the case, however, as 39% of all covalently trapped proteins (16 out of 41) represented known Rsp5 interactors. A possible explanation for these seemingly contradictory results is that the UBAITylated products of other cellular E3s would be distributed among a very large number of substrates, such that the signal from any given protein would be very low, whereas the signal from the covalently trapped Rsp5 substrates would be concentrated among a relatively small number of proteins. The fact that the Rsp5 WT and C-A UBAITs isolated a broad range of known interacting proteins (as did other UBAITs; below) implies that the potential use of the fusion proteins as a source of ubiquitin is not a significant impediment to the approach.

Itch UBAITs in human cells

Itch is one of nine human Nedd4 family HECT E3s. These E3s have many functions and binding partners in human cells and play a role in ubiquitin-mediated endocytosis and immune regulation [49,50]. TAP-Itch UBAITs (WT and ΔGG) were expressed by transfection in HEK293T cells to determine whether UBAITs could trap targets in human cells. Cell lysates were prepared 36 h post-transfection, and conjugates were purified on IgG sepharose. An anti-TAP immunoblot showed a distribution of high molecular weight conjugates to the WT UBAIT, but not the ΔGG UBAIT (Appendix Fig S6). As with Rsp5, the ubiquitin moiety did not destabilize Itch in human cells (Appendix Fig S4B), and a distribution of conjugates emanated upward from the Itch WT UBAIT, but not the ΔGG. Total UBAIT conjugates were analyzed by mass spectrometry as described above for Rsp5. Three biological replicates of the experiment were performed.

Table 2 shows total spectral counts for proteins that co-purified specifically with the Itch WT UBAIT in all three replicates. Out of the 18 proteins that met the filtering criteria, seven were known Nedd4 family interactors (38%). These proteins included Stam and Hrs, which function in endosomal sorting complexes required for transport (ESCRT) pathway [50,51]. Alix, also part of the ESCRT pathway, was isolated, which has been reported to interact with other Nedd4 family members [52,53]. Wbp2, which interacts with the WW domains of Nedd4 family proteins, was also isolated [54]. Unlike the Rsp5 UBAITs, there were no proteins that co-purified with both the WT and the ΔGG Itch UBAITs.

RING E3 UBAITs

The results presented above indicated that the Rsp5 UBAITs trapped targets in cells via a non-lariat mechanism, independent of the HECT catalytic cysteine. This suggested that the approach could be applied to other types of E3s, including RING E3s, which do not function via a thioester intermediate. This was first tested with Psh1, a yeast RING E3. Psh1 is responsible for ubiquitylation of Cse4/CENP-A, a histone H3 variant. Cse4 is normally localized to centromeric chromatin, and it is ubiquitylated and degraded when it is mislocalized to euchromatin [55,56]. Cse4 is so far the only known substrate of Psh1. It was also recently shown that Psh1 interacts with Spt16, a component of the FACT (Facilitates Chromatin Transcription/Transactions) complex, and that this interaction is necessary for Psh1 to ubiquitylate Cse4 in cells but not *in vitro* [57]. To determine whether the Psh1 UBAIT was capable of covalently trapping Cse4 *in vitro*, Psh1 UBAITs (WT and ΔGG) were combined with E1 and E2 (Ubc1) proteins and ^{32}P-labeled Cse4. As predicted, the WT UBAIT, but not the ΔGG, formed a covalent conjugate to Cse4 (Appendix Fig S7A).

TAP-tagged Psh1 UBAITs (WT and ΔGG) were expressed in yeast. TAP-Psh1 UBAITs were expressed at similar levels to TAP-Psh1, indicating that the ubiquitin moiety did not result in destabilization of the fusion protein (Appendix Fig S4C). Conjugates were purified and analyzed as described above. Three biological replicates were performed, and a total of 15† proteins were common to all three replicates (Table 3). As predicted, both Cse4 and Spt16 were isolated specifically with the WT Psh1 UBAIT, but not the ΔGG UBAIT. Two other histone proteins (H3 and H4) were also isolated. While these are not thought to be ubiquitylated by Psh1, they have been shown previously to co-immunoprecipitate with Psh1, likely as a result of their indirect association with Cse4 in nucleosome complexes [56]. Their covalent "trapping" to Psh1 may therefore reflect their proximity to Cse4 in nucleosome complexes. Two proteasome proteins were also trapped (Rpn10 and Pup3), although the significance of this is not known. It should be noted that while the spectral counts for both Spt16 and Cse4 were very low, the fact that both proteins were identified in three independent experiments points to the specificity and sensitivity of the UBAIT method for profiling RING E3s.

RNF126 is a human RING ubiquitin ligase involved in degradation of mislocalized and aggregation-prone proteins. This pathway is dependent on the interaction of RNF126 with the Bag6 complex

†Correction added on 2 December 2015 after first online publication: the number "14" has been corrected to "15".

Table 2. Itch UBAIT targets identified in human 293T cells.

			Experiment 1			Experiment 2			Experiment 3			
ACC#	Protein	MW [kDa]	WT	ΔGG	TAP	WT	ΔGG	TAP	WT	ΔGG	TAP	PY-like motif
Q8WUM4	**ALIX**	**96.0**	**31**	**0**	**0**	**32**	**0**	**0**	**35**	**0**	**0**	yes
P39060-2	COL18A1	135.7	17	37	0	3	74	0	20	62	0	yes
F8WJN3	CPSF6	52.2	17	17	0	23	13	0	41	26	5	yes
Q9UBN7	HDAC6	131.3	59	0	0	85	0	0	71	0	0	no
O14964	**HRS**	**86.1**	**78**	**0**	**0**	**53**	**0**	**0**	**57**	**0**	**0**	yes
P52292	KPNA2	57.8	216	0	0	295	0	0	189	0	0	no
H7C3B6	LRRK2	23.0	17	22	0	7	37	0	12	15	0	yes
P12004	PCNA	28.8	8	0	0	17	0	0	12	0	0	no
P24928	**POLR2A**	**217.0**	**1,782**	**3,086**	**2**	**555**	**3,727**	**0**	**702**	**1,840**	**85**	yes
O14828	**SCAMP3**	**38.3**	**18**	**0**	**0**	**27**	**0**	**0**	**19**	**0**	**0**	yes
Q15758	SLC1A5	56.6	10	0	0	16	1	0	12	0	0	no
P08195-2	SLC3A2	57.9	13	0	0	7	0	0	13	0	0	yes
Q92783-2	**STAM**	**44.9**	**54**	**0**	**0**	**30**	**0**	**0**	**39**	**0**	**0**	yes
P22314	UBA1	117.8	134	0	0	234	3	5	132	0	0	yes
A0AVT1	UBA6	117.9	106	0	0	127	0	0	95	0	0	no
P45974-2	USP5	93.2	13	0	0	36	0	0	27	0	0	yes
Q93008-1	USP9X	290.3	16	1	0	19	10	0	25	13	4	yes
K7EIJ0	**WBP2**	**18.2**	**67**	**0**	**0**	**70**	**0**	**0**	**68**	**0**	**0**	yes
Q9H0M0-6	**WWP1**	**81.6**	**606**	**177**	**0**	**760**	**640**	**11**	**430**	**339**	**18**	yes

Total spectral counts of targets identified with Itch WT UBAIT, ΔGG UBAIT, and empty TAP control (TAP). Experiment was performed in triplicate. Data was filtered according to the following parameters: proteins with four or more spectral counts for the WT sample and greater than or equal to five-fold more counts in WT sample compared to TAP control. Identified proteins were analyzed for the presence of PY-like motifs [94]. Known Nedd4 family binding partners are shown in bold.

(Bag6/Trc35/Ubl4A) [58]. To determine whether the RNF126 UBAIT was capable of covalently trapping Bag6 *in vitro*, RNF126 UBAITs (WT and ΔGG) were combined with E1 and E2 (Ubc1) proteins and a ^{32}P-labeled truncated form of Bag6 (amino acids 1–167). As predicted, the WT UBAIT, but not the ΔGG UBAIT, formed a stable covalent conjugate to Bag6 (Appendix Fig S7B). As seen with Rsp5, a higher molecular weight conjugate above the expected single WT UBAIT-target conjugate was observed and corresponds in size to a di-UBAITylated Bag6 molecule. RNF126 UBAIT conjugates were purified from transfected HEK293T cells (Appendix Fig S4D). As shown in Appendix Table S4, the RNF126 WT UBAIT trapped Bag6 in three biological replicates, and the spectral counts were among the highest of all the proteins isolated [58,59]. The other two components of the Bag6 complex (Trc35, Ubl4A) were not isolated, possibly because of their relative proximity to RNF126 in the Bag6 complex. Many additional proteins were also isolated with the WT UBAIT, which may reflect the large number of quality control substrates of the Bag6 complex.

We further tested the ability of UBAITs to identify RING E3 targets using human RNF168. RNF168 is a key mediator of DNA double-strand break signaling and repair [60,61], and RNF168 mutations are associated with Riddle syndrome, a human disorder characterized by immunodeficiency and radiosensitivity [62–64]. TAP-RNF168 and TAP-RNF168 UBAITs (WT and ΔGG) were expressed by transfection in HEK293T cells (Fig 3A). Immunoblotting confirmed expression of all three proteins and formation of conjugates to only the WT UBAIT (Fig 3B). Transfected cells were treated with ionizing radiation, and purification and mass spectrometry analysis of the UBAITS identified histone H2A only in the WT UBAIT sample (Table 4). Ubiquitylation of H2A by RNF168 is a vital signaling event in the DNA damage response and represents the most well-established target of RNF168 [65,66]. In addition, histone H2AZ, a member of the H2A family of histone variants, was identified as a potentially novel RNF168 substrate. H2AZ is recruited to sites of DSBs to facilitate repair by non-homologous end joining [67]. To validate H2AZ as a target, we first overexpressed RNF168 in HEK293T cells. This led to an additional H2AZ ubiquitylation product of H2AZ, beyond the previously characterized monoubiquitylated species generated by the RING1B ligase (Fig 3C) [68]. RNF168 also ubiquitylated H2AZ *in vitro* in H2AZ-containing reconstituted nucleosome core particles (NCPs) (Fig 3D). The D94A mutation in H2AZ disrupts an acidic patch that is required for repair activity. The analogous mutation in H2A blocks recruitment of RNF168 to nucleosomes [69], and this mutation also prevented *in vitro* ubiquitylation of H2AZ in NCPs (Fig 3D). Together, these results validate H2AZ as a target of RNF168 and demonstrate the utility of the UBAIT approach for identification of novel ubiquitin ligase targets.

Discussion

In vitro and *in vivo* results presented here validate Ubiquitin-Activated Interacting Traps (UBAITs) as useful tools for identification

Table 3. Proteins identified in Psh1 UBAITs in *Saccharomyces cerevisae*.

			Experiment 1			Experiment 2			Experiment 3		
ACC#	Protein	MW [kDa]	WT	ΔGG	TAP	WT	ΔGG	TAP	WT	ΔGG	TAP
P19454	CKA2	39.4	6	0	0	26	0	0	8	0	0
P36012	**CSE4**	**26.8**	**5**	**0**	**0**	**4**	**0**	**0**	**4**	**0**	**0**
P34216	EDE1	150.7	4	0	0	2	0	0	2	0	0
P02309	HISTONE H4	11.4	5	0	0	5	0	0	3	0	0
P61830	HISTONE H3	15.3	19	0	0	29	0	0	33	3	0
P02293	HISTONE H2B	14.2	5	0	0	5	0	0	9	0	0
P25369	LSB5	39.8	3	0	0	4	0	0	4	0	0
Q12499	NOP58	56.9	2	2	0	2	1	0	6	3	0
P25451	PUP3	22.6	5	0	0	4	0	0	3	0	0
Q02792	RAT1	115.9	3	0	0	2	0	0	2	0	0
P03872	REP2	33.2	9	0	0	7	0	0	4	0	0
P10964	RPA190	186.3	13	2	0	25	18	1	29	14	1
P38886	RPN10	29.7	3	0	0	2	0	0	2	0	0
P32790	SLA1	135.8	70	24	0	20	1	0	25	3	0
P32558	**SPT16**	**118.6**	**23**	**0**	**0**	**13**	**0**	**0**	**9**	**0**	**0**

Total spectral counts for proteins common to all three biological replicates of Psh1 WT UBAIT, ΔGG UBAIT, and empty TAP control (TAP). Data were filtered according to the following parameters: proteins with two or more spectral counts for the WT sample and greater than or equal to five-fold more counts in WT sample compared to TAP control. Known Psh1-interacting partners are shown in bold.

of substrates and other interacting proteins for both HECT and RING ubiquitin ligases. While the approach was conceived to be specific for HECT ubiquitin ligases (e.g., Rsp5 and Itch), the lack of dependence on the active-site cysteine suggested that the same approach could be applied to RING ubiquitin ligases, and this was validated with three different RING E3s (Psh1, RNF126, and RNF168). Furthermore, the RNF168 UBAIT identified histone H2AZ as a new target of this E3.

Thirty percent of the proteins that were isolated with the Rsp5 UBAIT and passed filtering criteria were known Rsp5-interacting proteins, and these represented approximately 32% of all proteins reported to interact with Rsp5 (Appendix Table S5). Of the known interacting proteins that were covalently trapped by the Rsp5 WT and C-A UBAITs in yeast cells, many were substrate adaptor proteins, including six out of the ten Art proteins [70], rather than classical ubiquitylation substrates. For example, Art5 was trapped, but the Rsp5/Art5 target, Itr1 [71], was not. Art1 was also trapped, and while the Rsp5/Art1 target Mup1 was trapped, Can1 and Lyp1 were not [70]. A bias toward adaptor proteins might simply reflect the steady-state distribution of Rsp5 with its associated proteins in cells. Also, the yeast experiments reported here were performed under standard growth conditions, and the lack of identification of some targets might reflect the physiologic state of the cells. For example, the ubiquitylation of Fur4 by Rsp5 occurs predominantly under nutrient deprivation [72,73].

Several potential novel targets of Rsp5 were also identified. Bmh2, a 14-3-3 protein, which has previously been shown to regulate the Rsp5 adaptor Bul1 [74], was isolated, and Ino1 (inositol 3-phosphate synthase) and Pdi1 (a protein disulfide isomerase) were also previously isolated in large-scale proteomic analyses of Rsp5-associated proteins [75,76]. Sul2 (a sulfur permease), two plasma membrane-associated t-SNAREs (Sso1 and Sso2), and Rvs161, a lipid raft protein, were also isolated, consistent with the role of Rsp5 in membrane protein trafficking. Other membrane-associated interacting proteins included Vti1 and Sac1, which are Golgi membrane proteins, and Pil1, which is localized to the mitochondrial membrane [77–79].

Endocytic pathway proteins were well represented among the Itch UBAIT conjugates in human cells, including Alix and SCAMP3, which have been reported to interact with other Nedd4 family members [52,53]. Expression of Itch UBAITs in other cell types may yield target proteins related to the function of Itch in immune regulation. For example, Bcl-10, JunB, and Cbl-b, which were not isolated with the Itch UBAIT, are Itch targets that play a role in immune responsiveness [80–83].

The UBAIT approach with RING E3s was validated with yeast Psh1 and human RNF126 and RNF168. Psh1 associates with Spt16, and this interaction is required for recognition and ubiquitylation of Cse4/CENP-A [57]. The UBAIT trapped both Spt16 and Cse4, the only two known interactors of Psh1, which points to the sensitivity and specificity of the approach. The Psh1 UBAIT also trapped other histone proteins, which may reflect the proximity of those proteins to Cse4 in nucleosome complexes. This highlights the potential usefulness of UBAITs as tools to map intracellular locale or proximity to other proteins. While the RNF126 UBAIT trapped its best-characterized associated protein, Bag6, it also trapped a large number of previously uncharacterized RNF126-interacting proteins. We speculate that at least some of these may reflect quality control client proteins of the Bag6/RNF126 complex [58]. The RNF168 UBAIT trapped histone H2A, the best-characterized substrate of this ligase, as well as H2AZ, a previously unknown substrate of RNF168. The nucleosome acidic patch region of H2AZ was required for

Published online: October 27, 2015
EMBO reports

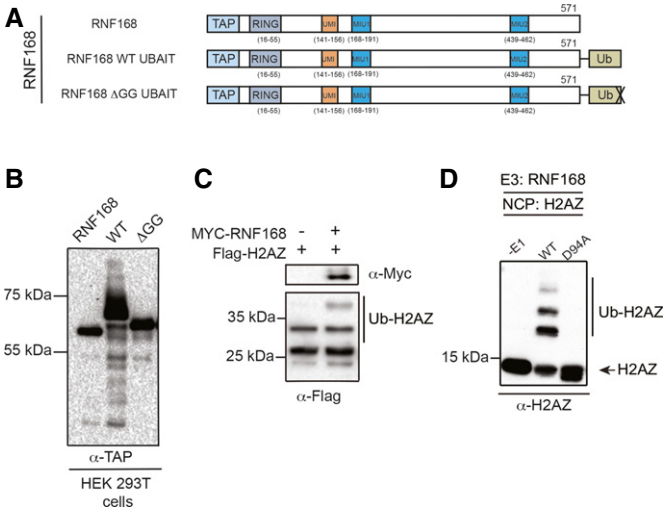

Figure 3. RNF168 UBAIT traps histone H2AZ in cells and *in vitro*.

A Depiction of wild-type RNF168, RNF168 UBAIT (WT), and ΔGG ubiquitin (ΔGG) UBAIT. The structural positions of the ubiquitin binding domains (UBDs) MIU (motif interacting with ubiquitin), UMI (UIM- and MIU-related UBD), and RING domains are indicated.

B Immunoblot (anti-TAP) of extracts from human HEK293T cells expressing TAP-RNF168 or the indicated TAP-RNF168 UBAITs.

C Ubiquitylation of FLAG-H2AZ in HEK293T cells transiently transfected with FLAG-H2AZ in the presence and absence of MYC-RNF168 (lanes 1 and 2, respectively; lower panel). Expression of MYC-RNF168 was verified by anti-MYC immunoblotting (upper panel).

D Purified H2AZ-containing reconstituted nucleosome core particles (NCPs) were used in an *in vitro* ubiquitylation assay in the presence of RNF168. WT H2AZ-containing NCPs (first two lanes) were incubated with RNF168, UBCH5a, and ubiquitin, without or with E1 enzyme (lanes 1 and 2, respectively). Third lane contains D94A-containing NCPs, incubated with RNF168, UbcH5a, ubiquitin, and E1.

RNF168-dependent ubiquitylation, and although this region has been shown to promote ubiquitylation of H2A [66,69,84,85], H2AZ contains an extended acidic patch which may confer unique structure and function to H2AZ compared to other H2A family members [86].

The potential to capture potentially weak and transient protein–protein interactions is a key feature of the UBAIT approach. Other approaches for characterizing E3s have been recently reported, including one that fuses UBA ubiquitin binding domains to F-box proteins to capture the product of F-box protein-mediated ubiquitylation events [34]. While the UBA fusion approach was designed to specifically characterize ubiquitin ligases, the UBAIT approach is not necessarily limited to characterizing ubiquitin ligases. It has the potential to be used as a general protein–protein interaction tool, where virtually any protein of interest (POI) could be fused to ubiquitin as a way of trapping its interacting partners. This assumes that the POI does not have to be a ubiquitin ligase in order to trap interacting proteins, and preliminary experiments with RING UBAITs deleted of the RING domain suggest this is the case (H.F. O'Connor and J.M. Huibregtse, unpublished observation). Similar to the UBAIT concept, the "NEDDylator" system and the BioID biotinylation-based proximity ligation approaches can potentially be adapted for any POI [33,34]. The NEDDylator is a POI-Ubc12 fusion protein, which can be added to cell lysates or expressed in cells along with a tagged form of NEDD8. A subsequent tagged NEDD8 immunoprecipitation identifies NEDDylated conjugates, including the targets of the POI. In the BioID system, the addition of exogenous biotin and a promiscuous BirA-POI fusion protein biotinylates proximal binding partners. The principal advantage of the UBAIT method over these is that the reaction product is covalently trapped to the POI, as opposed to being a reaction product that is no longer in complex with the bait protein; this may increase the confidence that a target protein was indeed trapped as a result of close proximity to the bait protein.

The UBAIT system may be further optimized by modification of either the linker peptide connecting the POI to ubiquitin or the purification epitope. While we have not yet observed significantly different outcomes based on linker length or linker sequence for HECT or RING UBAITs, it is conceivable that specific UBAITs might have unique requirements. The UBAITs described here have an N-terminal purification epitope in addition to the C-terminal linker-ubiquitin epitope. Incorporation of the affinity purification into or adjacent to the linker sequence would allow one-step C-terminal epitope tagging which would be useful for genomic tagging of individual genes in yeast or human cells. Finally, while HECT E3s share a common architecture, with the HECT domain located at the C-terminus of the protein, monomeric RING E3s are structurally very diverse. Of the three RING E3s examined here, two have their RING domain at their extreme N-terminus (Psh1 and RNF168), while the RING domain of RNF126 is located near the C-terminus of the protein. The fact that all three RING UBAITs successfully isolated interacting proteins suggests that UBAIT functionality is not limited in any obvious way by domain

Table 4. Proteins identified in RNF168 UBAIT samples in human 293T cells.

			Experiment 1			Experiment 2			Experiment 3		
ACC#	Protein	MW [kDa]	WT	ΔGG	TAP	WT	ΔGG	TAP	WT	ΔGG	TAP
Q9H1R3	MYLK2	64.6	20	62	2	47	49	3	43	36	8
P12004	PCNA	28.8	18	0	0	28	0	0	12	0	0
P0C0S5	HISTONE H2AFZ	13.5	17	1	0	6	0	0	19	2	0
P04908	HISTONE H2A type 1-B/E	14.1	12	0	0	22	1	0	28	1	1

Total spectral counts of targets identified with RNF168 WT UBAIT, ΔGG UBAIT, and empty TAP control (TAP) following ionizing radiation treatment. Experiment was performed in triplicate. Data were filtered according to the following parameters: proteins with four or more spectral counts for the WT sample and greater than or equal to five-fold more counts in WT sample compared to TAP control (see Appendix Table S4 for complete unfiltered data). Identified proteins were analyzed for the presence of PY-like motifs [94].

organization of the protein of interest. In summary, we have developed a novel approach for characterizing proteins that interact with HECT and RING ubiquitin ligases. The "trapping" aspect of this approach is likely to be particularly important when applied to ligases and other classes of enzymes or proteins that engage in weak or transient protein–protein interactions.

Materials and Methods

DNA constructs and recombinant protein expression

Escherichia coli expression vectors and the production of Ubc1, Sna3–K125, Sna3–PAAA, and wild-type Rsp5 and Wbp2 proteins were previously described [40,87,88]. The MYC-RNF168 construct was previously described [69], and bacterial expression vectors for core histones (human H2B, H3, and H4) in pET21 and pPROEX HTa-RNF168 (residues 1–113) were previously described [89]. Itch was PCR-amplified from *Mus musculus* cDNA. Itch UBAITs, Rsp5 $(GA)_6$-repeating dipeptide UBAITs, and Psh1 UBAITs were generated by overlap extension PCR. Rsp5 $(GGSG)_{1, 3, 5,}$ were generated by homologous recombination in *Saccharomyces cerevisiae* strain FY56 (MATα *his4-912δR5 lys2-128δ ura3-52)* [45]. RNF126 UBAITs were generated using the one-step cloning vector for generating E3-Ub fusion proteins (Appendix Fig S8). Further cloning information and primer sequences are provided below.

ORFs were sub-cloned into pGEX-6p-1 and pGEX-6p-K for bacterial expression of GST fusion proteins [40], and were sub-cloned into pYES2-NTAP or pcDNA3-TAP for *in vivo* expression in yeast and human cells, respectively [87,90]. pYES2-NTAP constructs were transformed into *S. cerevisiae* FY56. GST fusion proteins were expressed in *E. coli* by standard methods and affinity-purified on Glutathione-Sepharose beads (GE Healthcare). Proteins expressed from pGEX-6p-1 vector were cleaved from GST by using PreScission protease (GE Healthcare) under manufacturer-recommended conditions, and these proteins were used in ubiquitin-thioester and ubiquitylation reactions. The His_6-tagged RNF168 (1–113) construct was expressed in Rosetta 2 (DE3) pLysS cells and purified over a Ni-NTA column (Qiagen) as described [69].

Overlapping extension PCR

Rsp5 $(GA)_6$ UBAIT WT and ΔGG were generated by overlapping PCR. Using Rsp5 wild-type and C-A mutant plasmids as template [91], round 1A product was generated with primers Rsp5F (GGGG AA TTCATG CCTTCA TCCATA TCCGTC AA) and Rsp5UbGA6R (CCCGCT CCAGCC CCCGCA CCGGCG CCTTCT TGACCA AACCCT ATG). Using yeast ubiquitin as template, round 1B product (yeast ubiquitin wild-type or ΔGG mutant) was generated with Rsp5UbGA6F (GCTGGA GCGGGT GCAGGG GCCCAG ATTTTC GTCAAG ACTTTG) and yUbWTR (GGGGCG GCCGCT CAACCA CCTCTT AGCCTT AGC) or yUbGGR (GGGGCG GCCGCT CATCTT AGCCTT AGCACA AGA), respectively. Round 2 PCR product was generated using 1A and 1B as template and primers Rsp5F and yUbWTR or yUbGGR to generate Rsp5 $(GA)_6$ UBAIT WT (or C-A mutant) and Rsp5 $(GA)_6$ UBAIT ΔGG, respectively.

Similarly, Psh1 UBAIT WT and ΔGG were constructed by overlapping PCR. For round 1A PCR, Psh1 was amplified from *S. cerevisae FY56* genomic DNA using PSH1F (GGGGAA TTCATG GGCGAC GAATTA CACAAC CG) and PSH1UbLX1R (CCAGAT CCGCCT TCATCG TCACTG TCTCCT AG) (round 1A, Psh1). Round 1B (yeast ubiquitin wild-type or ΔGG mutant) was generated with PSH1F (CCAGAT CCGCCT TCATCG TCACTG TCTCCT AG) and yUbWTR or yUbGGR, respectively. Round 2 PCR was generated using 1A and 1B as template and primers PSH1F and yUBWTR or yUBGGR to generate Psh1 UBAIT WT and Psh1 UBAIT ΔGG, respectively.

Itch UBAIT WT and ΔGG were generated using ITCHF (CCGGAT CCTCTG ACAGTG GACCAC AGCTT) and ITCHUBLX1R (GGTCTT CACGAA GATCTG ACCAGA ACCACC CTCTTG TCCAAA TCCTTC) (round 1A) and ITCHUBLX1F (GAAGGA TTTGGA CAAGAG GGTGGT TCTGGT CAGATC TTCGTG AAGACC) with hUbWTR (GGGCGG CCGCTC AACCAC CTCTGA GACGG) or hUbGGR (GGGCGG CCGCTC ATCTGA GACGGA GGACCA GG) (round 1B, human ubiquitin wild-type or ΔGG mutant, respectively). Round 2 PCR was generated using 1A and 1B as template and primers ITCHLX1F and hUbWTR or hUbGGR to generate Itch UBAIT WT and Itch UBAIT ΔGG, respectively.

Homologous recombination

Rsp5 $(GGSG)_{1, 3, 5}$ UBAITs WT and ΔGG were generated by homologous recombination in a two-round process with the pYES2-NTAP vector in *S. cerevisae*. Firstly, wild-type or ΔGG mutant ubiquitin PCR product was amplified with GGSG-encoding oligonucleotides at the 5′ end and 30–60 bp overhangs complementary to the desired site of recombination in pYES2-NTAP at the 5′ end (R1LX1F (CCTCCG GGGCAC TTGATG ATGACG ATCCCG GGGGCG GATCTG GTCAGA TTTTCG TCAAGA CTTTG), R1LX3F (AAATCT CATCCT CCGGGG CACTTG ATGATG ACGATC CCGGGG GCGGAT CTGGTG GCGGAT CTGGTG GCGGAT CTGGTC AGATTT TCGTCA AGACTT TGACC), and R1LX5F (TCTCAT CCTCCG GGGCAC TTGATG ATGACG ATCCCG GGGGCG GATCTG GTGGTG GGAGCG GCGGGG GTTCGG GAGGAG GGTCCG GTGGGG GTTCG) for $(GGSG)_{1, 3, 5}$, respectively) and 3′ end (R1WTUBR (TGAATG TAAGCG TGACAT AACTAA TTACAT GATGCG GCCCTC AACCAC CTCTTA GCCTTA GCACAA G) or R2GGUbR (GTAAGC GTGACA TAACTA ATTACA TGATGC GGCCCT CATCTT AGCCTT AGCACA AGATGT AAG) for wild-type and ΔGG ubiquitin, respectively). Restriction digest of 100 ng pYES2-NTAP with BglII was performed overnight and transformed, along with 600 ng of GGSG-Ub PCR product [92]. Following selection on SC-URA agar plates, DNA was extracted from yeast cells. Positive clones were verified by electroporation of the yeast plasmid DNA into *E. coli*, followed by sequence analysis. In a second round, Rsp5 was amplified by PCR along with overhangs complementary to pYES2-NTAP at the 5′ end (R2RSP5F (GAAAAT CTCATC CTCCGG GGCACT TGATGA TGACGA TATGCC TTCATC CATATC CGTCAA GTTAGT GG) for GGSG-ubiquitin) and at the 3′ end (R2RSP5LX1R (GGTCAA AGTCTT GACGAA AATCTG ACCAGA TCCGCC TTCTTG ACCAAA CCCTAT GGTTTC TTCC) and R2RSP5LX3R (CTGACC AGATCC GCCACC AGATCC GCCACC AGATCC GCCTTC TTGACC AAACCC TATGGT TTCTTC C) for $(GGSG)_{1, 3}$, respectively). Rsp5 $(GGSG)_5$ UBAIT was generated using pYes2-NTAP Rsp5 $(GGSG)_3$ UBAIT WT as template, using R2RSP5LX5F (TCTCAT CCTCCG GGGCAC TTGATG ATGACG ATCCCG GGGGCG GATCTG GTGGTG GGAGCG GCGGGG GTTCGG GAGGAG GGTCCG GTGGGG GTTCG) and R2RSP5LX5R (ACCAGA TCCGCC ACCAGA TCCGCC ACCAGA

TCCGCC ACCACT TCCACC TCCCGA ACCCCC ACCGGA CCCTCC TCCCGA ACC).

One-step UBAIT cloning vector

A one-step cloning vector was constructed to allow a UBAIT to be constructed with one round of PCR and ligation. Wild-type and ΔGG mutant ubiquitin were amplified using UBVX1F (AATAAT GCGGCC GCAGGC GGATCT GGTCAG ATTTTC GTCAAG ACT) and UBWTVX1R (CTTCTT TCTAGA TCAACC ACCTCT TAGCCT TAGCAC AAGATG TAAGG) or ubGGVX1R (CTTCTT TCTAGA TCATCT TAGCCT TAGCAC AAGATG TAAGGT GGACTC C), respectively. Following NotI-XbaI restriction digest, the PCR product was cloned in to pcDNA3-TAP to make pcDNA3-TAP-VX1UbWT and pcDNA3-TAP-VX1UbGG. The vector allows the protein of interest to be cloned with the restriction sites 5′ to NotI, such as BamHI and EcoRI at the 5′ end and NotI at the 3′ end to yield a POI-AAAGGSG-Ub fusion protein. The RNF126 UBAIT WT and RNF126 UBAIT ΔGG were generated by amplifying RNF126 by PCR from HEK293T cDNA with RNF126VX1F (ATAGTC GAATTC ATGGCC GAGGCG TCGCCG CA) and RNF126VX1R (GAGCTA GCGGCC GCCGAG TTGCTT GTGGCG TTCTCG TTGCTG GG) and cloning into pcDNA3-TAP-UbVX1WT and pcDNA3-TAP-UbVX1GG. The RNF168 UBAIT WT and RNF168 UBAIT ΔGG were generated by amplifying RNF168 by PCR from HEK293T cDNA with RNF168VX1F (TTTGAA TCCATG GCTCTA CCCAAA GACGCC) and RNF168VX1R (TTTGCG GCCGC C TTTGTG CATCTC TGAAAC) and cloning into pcDNA3-TAP-UbVX1WT and pcDNA3-TAP-UbVX1GG. The internal EcoRI restriction digestion site present in RNF168 coding gene was initially mutated using RNF168MUTF (GTATCT CGGCTT CTCCCT TAAACT CCAGAA AATCTG ATCCAG) and RNF168MUTR (CTGGAT CAGATT TTCTGG AGTTTA AGGGAG AAGCCG AGATAC).

Construction of non-UBAIT-encoding plasmids

Cse4 was amplified by PCR from *S. cerevisae* genomic DNA using Cse4F (GGGAAT TCATGT CAAGTA AACAAC AATGG) and Cse4R (GGGCGG CCGCCT AAATAA ACTGTC CCCTGA TTC) to generate pGEX-6p-K-Cse4. Bag6 was amplified by PCR from HEK293T cDNA using Bag6F (ATAGTC GAATTC ATGGAG CCTAAT GATAGT ACCAG) and Bag6R (CATGTA GCGGCC GCACCA GCCGTA CCCGG) to generate pGEX-6p-K-Bag6 (1–167 amino acids).

RNF126 (no Ub fusion) was generated by amplifying RNF126 by PCR from HEK293T cDNA with RNF126VX1F (ATAGTC GAATTC ATGGCC GAGGCG TCGCCG CA) and RNF126R (GAGCTA GCGGCC GCTCAC GAGTTG CTTGTG GCGTTC TCGTTG CTGGG) and cloning into pcDNA3-TAP. Itch (no Ub fusion) was generated by PCR with ITCHF (CCGGAT CCTCTG ACAGTG GACCAC AGCTT) and ITCHR (GGGCGG CCGCTT ACTCTT GTCCAA ATCCTT) and cloning into pcDNA3-TAP. Psh1 (no Ub fusion) was generated by PCR from *S.cerevisae* FY56 genomic DNA using PSH1F (GGGGAA TTCATG GGCGAC GAATTA CACAAC CG) and PSH1R (GGGGCG GCCGCT TATTCAT CGTCAC TGTCTC C) and cloning into pYES2-NTAP.

Human H2AZ cDNA was cloned into a N-terminal FLAG-tagging vector using Gateway LR reaction. Human H2AZ cDNA was cloned using H2AZF (ATGGCT GGCGGT AAGGCT GG) and H2AZR (TTAGAC AGTCCT CTGTTG TCC) into Gateway compatible entry vector (pDONR201) and subcloned into bacterial expression vector pDEST17 harboring N-terminal 6× His tag. 5′-biotin-tagged 601 nucleotide sequence to be used for reconstitution of nucleosomes was generated as previously described [69].

Mutations in H2AZ (for D94A) were generated by site-directed mutagenesis following standard protocols with H2AZD94AF (GCAACT TGCTAT TCGTGG AGCTGA AGAATT GGATTC TCTC) and H2AZD94AR (GAGAGA ATCCAA TTCTTC AGCTCC ACGAAT AGCAAG TTG).

Biochemical assays

Ubiquitin-thioester reactions were performed as described previously [87]. Reaction mixtures were incubated for 15 min for thioester assays at room temperature. For substrate ubiquitylation assays, ^{32}P-labeled proteins, generated as described previously [40], were incubated with 5 μg/ml of Rsp5 or Rsp5 UBAIT in the presence of 25 mM Tris–HCl (pH 7.5), 50 mM NaCl, 5 mM $MgCl_2$, 0.1 mM DTT, 50 μg/ml of ubiquitin (Sigma), 1.25 μg/ml of human E1 (Boston Biochem), 1.25 μg/ml of Ubc1 (40 μl total volume), and 10 mM ATP. All reactions were initiated by the addition of ubiquitin or UBAIT and stopped by the addition of 4×SDS–PAGE loading buffer either lacking or containing 0.4 M DTT. Reaction mixtures were incubated for 1 h at room temperature. Ubiquitylated products were analyzed using Typhoon FLA 9500 (GE Healthcare).

For RNF168 *in vitro* ubiquitylation assays, 2.5 μg of recombinant mononucleosomes was incubated in a 50-μl reaction buffer containing 50 μM Tris–HCl, pH 7.5, 100 mM NaCl, 10 mM $MgCl_2$, 1 μM ZnOAc, 1 mM DTT, 30 nM ubiquitin-activating enzyme E1 (Boston Biochem), 1.5 μM ubiquitin-conjugating enzyme UbcH5a (Boston Biochem), 4 μM RNF168 (1–113), 22 μM ubiquitin (Boston Biochem), and 3.33 mM ATP at 30°C for 4 h [69].

Two-step TAP-tagged protein purification in yeast cells

For Rsp5 UBAITs, 200 ml of overnight cultures was diluted to 1.5 l with synthetic complete medium without uracil (SC-Ura) and with 2% sucrose. After 3 h at 30°C, 2% galactose was added, and cultures were incubated for an additional 3 h. Cells were pelleted at 3,210 × *g* for 5 min and then lysed in 800 μl NP-40 lysis buffer (1% Nonidet P-40, 100 mM Tris, pH 7.9, 100 mM NaCl, 1 mM DTT, 100 μM phenylmethylsulfonyl fluoride, 4 μM leupeptin, 0.3 μM aprotinin, and 10 mM N-ethylmaleimide) by bead beating for six cycles for 2 min (2 min on ice between cycles). About 10 ml of RIPA buffer (50 mM Tris pH 7.4, 150 mM NaCl, 1% NP-40, 0.1% SDS, 0.5% sodium deoxycholate, 1 mM DTT, 100 μM phenylmethylsulfonyl fluoride, 4 μM leupeptin, 0.3 μM aprotinin, and 10 mM N-ethylmaleimide) was added to the lysate and the lysate cleared by centrifugation at 4°C for 20 min. For the first round of purification, cell lysate was transferred to a new tube and immunoprecipitated with 300 μl IgG sepharose beads (GE Healthcare) at 4°C for 2 h. Beads were collected by gentle centrifugation and washed three times with RIPA buffer. About 200 μl denaturation buffer (20 mM TRIS, pH 8, 50 mM NaCl, 5 mM DTT, 1% SDS) was added to the beads, and samples were boiled at 95°C for 5 min. About 1 ml NP-40 wash buffer (0.1% NP-40) was used to wash the beads, and following centrifugation, the eluted proteins were transferred to a fresh tube with 10 ml NP-40 wash buffer (0.1%) and 300 μl fresh IgG sepharose beads for a second round of purification. Beads were

collected by gentle centrifugation, and following three washes with RIPA buffer, the cells were pelleted, and 75 μl SDS–PAGE loading buffer was added to the beads. Beads were boiled at 95°C for 5 min. Samples were analyzed by SDS–PAGE (8% gel) and stained with Coomassie blue. In addition, a fraction of the material was reserved for an anti-TAP immunoblot. The gel section above the expected size of the UBAIT was excised and, along with the corresponding section in the TAP empty control, was subject to in-gel tryptic digestion and LC-MS/MS. This protocol was also followed for Psh1 UBAITs, except cells were grown to OD_{600nm} of 0.5 prior to the addition of 2% galactose.

TAP-tagged protein purification from human cells

For large-scale UBAIT purifications, ten 10-cm plates of 293T cells (3 μg DNA per 10 cm plate) were transfected with each plasmid construct. RNF168 samples were treated with 10 grays of ionizing radiation (Faxitron X-ray) prior to lysis. Cells were harvested, lysed, and pooled 36 h post-transfection in NP-40 lysis buffer. Cleared cell lysates were collected and diluted with 4 ml RIPA buffer. Conjugates were purified on IgG sepharose beads (GE Healthcare), binding at 4°C for 4 h. Beads were washed three times with high salt RIPA buffer (400 mM NaCl), followed by three times with RIPA buffer. Proteins were eluted from beads by adding SDS–PAGE loading buffer and boiling the samples at 95°C for 5 min, and the samples were analyzed by SDS–PAGE and stained with Coomassie blue. The gel section above the unconjugated UBAIT was excised from the gel, subject to in-gel tryptic digestion and LC-MS/MS.

Mass spectrometry

Samples were subject to in-gel digestion and protein identification using LC-MS/MS at the University of Texas at Austin Proteomics Facility as previously described, with minor adjustments [93]. Briefly, LC-MS/MS was carried out by reverse phase using a Dionex Ultimate 3000 Nano UPLC interfaced with a Thermo Orbitrap Elite mass spectrometer in positive mode. The LC utilizes an Acclaim PepMap 100 Nano-Trap column (75 μM × 2 cm, C18, 3 μM, 100 angstroms) with two Acclaim PepMap RSLC columns in tandem with each other: a 15-cm column (75 μM × 15 cm, C18, 2 μM, 100 angstroms) and a 25-cm column (75 μM × 15 cm, C18, 3 μM, 100 angstroms). A packed spray tip with 15 cm of C18 was utilized, and the total column resin length is 55 cm. Peptides were eluted from a linear gradient starting with 5–40% buffer B over a period of 120 min with a flow rate of 300 nl/min. MS spectra and MS/MS spectra were acquired via data-dependent acquisition, with the full-scan MS occurring in the Orbitrap at 120,000 resolution. The top 20 most intense precursor ions were then selected for MS/MS CID fragmentation and the product ions were detected in the ion trap, with a dynamic exclusion of 60 s.

Spectra were searched against the UniProt human database (Itch, RNF126 and RNF168) and UniProt yeast database (Rsp5 and Psh1) along with decoy databases using SEQUEST HT (Proteome Discoverer 1.4, Thermo Scientific). Fully tryptic peptides with up to 2 missed cleavages were considered. Mass tolerance filters of 10 ppm (MS1) and 0.8 Da (MS2) were applied. PSMs were filtered using Percolator (implemented in Proteome Discoverer) to control false discovery rates (FDR) to < 1% as determined using a reverse sequence decoy database.

Proteins with two or more spectral counts from the WT UBAIT sample and greater than or equal to five-fold higher spectral counts in the WT UBAIT sample compared to the TAP control were considered "positive hits" and potential Rsp5-interacting proteins. Hits that were common to unrelated UBAITs in yeast (Cpr1, Ddi1, Ecm21, histone H2B, Met4, Pal1, Pgk1, Uba1, Ubc1, Ubi4, Yhr097c) and human (Amot, Fam115a, Spg20) cells were not further considered as potential interactors. Raw data files are available at ProteomeXchange, accession number PXD002791.

NCP reconstitution

Recombinant human histones H2B, H3, and H4 were expressed in *Escherichia coli* BL21 (DE3)/RIL cells and purified as described [69]. Histone H2AZ was extracted from the soluble fraction. Octamers were refolded from purified histones by mixing the four histones in equimolar ratios (10% more of H2AZ/H2B relative to H3/H4), followed by dialysis into 2 M NaCl, and then purified on a Superdex 200 (16/60) size exclusion column (GE Healthcare). Nucleosome core particles (NCPs) were reconstituted by salt deposition and confirmed as previously described [69].

Western blot

Western blots were detected using Li-cor Odyssey Detection System (Li-cor Biosciences). For RNF168 experiments, ubiquitylated products were analyzed using ECL Prime Western blotting detection reagent (GE Healthcare).

Antibodies

TAP primary antibody: Rockland Immunochemicals Inc. P500-0005, TAP secondary immunofluorescent antibody: LI-COR Goat anti-rabbit IgG antibody, 926-32211.

Primary antibody rabbit anti-H2AZ (2718, Cell Signaling Technologies) and secondary antibody HRP-linked goat anti-rabbit IgG (7074, Cell Signaling Technologies).

Expanded View for this article is available online:
http://embor.embopress.org

Author contributions

The concept was developed by HFO and JMH, and experiments were performed by HFO, NL, JWL, PA, and CDS. The paper was written by HFO, KMM, and JMH.

Acknowledgements

We thank members of the Huibregtse and Miller laboratories for critical comments on the manuscript, Andre Bui for assistance with the analysis of mass spectrometry results, Maria Person and Christopher Yellman for helpful discussions and technical advice, and Li-Ya Chiu for RNF168 constructs. This work was supported by a grant to J.M.H. from the National Institutes of Health (GM103619). J.W.L. is funded by a Cancer Prevention Research Institute of Texas (CPRIT) postdoctoral training grant. K.M.M. received funding from CPRIT (R116) as a CPRIT scholar and was supported by start-up funds from UT Austin. LC-MS/MS experiments were performed by the Proteomics Facility, University of Texas at Austin, supported by CPRIT (RP110782).

Conflict of interest

The authors declare that they have no conflict of interest.

References

1. Li W, Bengtson MH, Ulbrich A, Matsuda A, Reddy VA, Orth A, Chanda SK, Batalov S, Joazeiro CAP (2008) Genome-wide and functional annotation of human E3 ubiquitin ligases identifies MULAN, a mitochondrial E3 that regulates the organelle's dynamics and signaling. *PLoS ONE* 3: e1487
2. Popovic D, Vucic D, Dikic I (2014) Ubiquitylation in disease pathogenesis and treatment. *Nat Med* 20: 1242 – 1253
3. Hershko A, Ciechanover A (1998) The ubiquitin system. *Annu Rev Biochem* 67: 425 – 479
4. Grabbe C, Husnjak K, Dikic I (2011) The spatial and temporal organization of ubiquitin networks. *Nat Rev Mol Cell Biol* 12: 295 – 307
5. Kleiger G, Mayor T (2014) Perilous journey: a tour of the ubiquitin-proteasome system. *Trends Cell Biol* 24: 352 – 359
6. Metzger MB, Hristova VA, Weissman AM (2012) HECT and RING finger families of E3 ubiquitin ligases at a glance. *J Cell Sci* 125: 531 – 537
7. Deshaies RJ, Joazeiro CAP (2009) RING domain E3 ubiquitin ligases. *Annu Rev Biochem* 78: 399 – 434
8. Soss SE, Klevit RE, Chazin WJ (2013) Activation of UbcH5c ~ Ub is the result of a shift in interdomain motions of the conjugate bound to U-box E3 ligase E4B. *Biochemistry* 52: 2991 – 2999
9. Pruneda JN, Littlefield PJ, Soss SE, Nordquist KA, Chazin WJ, Brzovic PS, Klevit RE (2012) Structure of an E3:E2 ~ Ub complex reveals an allosteric mechanism shared among RING/U-box ligases. *Mol Cell* 47: 933 – 942
10. Dou H, Buetow L, Sibbet GJ, Cameron K, Huang DT (2012) BIRC7–E2 ubiquitin conjugate structure reveals the mechanism of ubiquitin transfer by a RING dimer. *Nat Struct Mol Biol* 19: 876 – 883
11. Plechanovová A, Jaffray EG, Tatham MH, Naismith JH, Hay RT (2012) Structure of a RING E3 ligase and ubiquitin-loaded E2 primed for catalysis. *Nature* 489: 115 – 120
12. Momand J, Zambetti GP, Olson DC, George D, Levine AJ (1992) The mdm-2 oncogene product forms a complex with the p53 protein and inhibits p53-mediated transactivation. *Cell* 69: 1237 – 1245
13. Stremlau M, Perron M, Lee M, Li Y, Song B, Javanbakht H, Diaz-Griffero F, Anderson DJ, Sundquist WI, Sodroski J (2006) Specific recognition and accelerated uncoating of retroviral capsids by the TRIM5alpha restriction factor. *Proc Natl Acad Sci U S A* 103: 5514 – 5519
14. Kee Y, Huibregtse JM (2007) Regulation of catalytic activities of HECT ubiquitin ligases. *Biochem Biophys Res Commun* 354: 329 – 333
15. Huang L, Kinnucan E, Wang G, Beaudenon S, Howley PM, Huibregtse JM, Pavletich NP (1999) Structure of an E6AP-UbcH7 complex: insights into ubiquitylation by the E2-E3 enzyme cascade. *Science* 286: 1321 – 1326
16. Verdecia MA, Joazeiro CAP, Wells NJ, Ferrer JL, Bowman ME, Hunter T, Noel JP (2003) Conformational flexibility underlies ubiquitin ligation mediated by the WWP1 HECT domain E3 ligase. *Mol Cell* 11: 249 – 259
17. Ogunjimi AA, Briant DJ, Pece-Barbara N, Le Roy C, Di Guglielmo GM, Kavsak P, Rasmussen RK, Seet BT, Sicheri F, Wrana JL (2005) Regulation of Smurf2 ubiquitin ligase activity by anchoring the E2 to the HECT domain. *Mol Cell* 19: 297 – 308
18. Ingham RJ, Gish G, Pawson T (2004) The Nedd4 family of E3 ubiquitin ligases: functional diversity within a common modular architecture. *Oncogene* 23: 1972 – 1984
19. Chen HI, Sudol M (1995) The WW domain of Yes-associated protein binds a proline-rich ligand that differs from the consensus established for Src homology 3-binding modules. *Proc Natl Acad Sci U S A* 92: 7819 – 7823
20. Bedford MT, Chan DC, Leder P (1997) FBP WW domains and the Abl SH3 domain bind to a specific class of proline-rich ligands. *EMBO J* 16: 2376 – 2383
21. Ermekova KS, Zambrano N, Linn H, Minopoli G, Gertler F, Russo T, Sudol M (1997) The WW domain of neural protein FE65 interacts with proline-rich motifs in Mena, the mammalian homolog of *Drosophila* enabled. *J Biol Chem* 272: 32869 – 32877
22. Bedford MT, Frankel A, Yaffe MB, Clarke S, Leder P, Richard S (2000) Arginine methylation inhibits the binding of proline-rich ligands to Src homology 3, but not WW, domains. *J Biol Chem* 275: 16030 – 16036
23. Scheffner M, Werness BA, Huibregtse JM, Levine AJ, Howley PM (1990) The E6 oncoprotein encoded by human papillomavirus types 16 and 18 promotes the degradation of p53. *Cell* 63: 1129 – 1136
24. Scheffner M, Huibregtse JM, Vierstra RD, Howley PM (1993) The HPV-16 E6 and E6-AP complex functions as a ubiquitin-protein ligase in the ubiquitylation of p53. *Cell* 75: 495 – 505
25. Jiang YH, Armstrong D, Albrecht U, Atkins CM, Noebels JL, Eichele G, Sweatt JD, Beaudet AL (1998) Mutation of the Angelman ubiquitin ligase in mice causes increased cytoplasmic p53 and deficits of contextual learning and long-term potentiation. *Neuron* 21: 799 – 811
26. Scheffner M, Kumar S (2014) Mammalian HECT ubiquitin-protein ligases: biological and pathophysiological aspects. *Biochim Biophys Acta - Mol Cell Res* 1843: 61 – 74
27. Marín I, Lucas JI, Gradilla A-C, Ferrús A (2004) Parkin and relatives: the RBR family of ubiquitin ligases. *Physiol Genomics* 17: 253 – 263
28. Morett E, Bork P (1999) A novel transactivation domain in parkin. *Trends Biochem Sci* 24: 229 – 231
29. Wenzel DM, Lissounov A, Brzovic PS, Klevit RE (2011) UBCH7 reactivity profile reveals parkin and HHARI to be RING/HECT hybrids. *Nature* 474: 105 – 108
30. Smit JJ, Sixma TK (2014) RBR E3-ligases at work. *EMBO Rep* 15: 142 – 154
31. Stynen B, Tournu H, Tavernier J, Van Dijck P (2012) Diversity in genetic in vivo methods for protein-protein interaction studies: from the yeast two-hybrid system to the mammalian split-luciferase system. *Microbiol Mol Biol Rev* 76: 331 – 382
32. Gupta R, Kus B, Fladd C, Wasmuth J, Tonikian R, Sidhu S, Krogan NJ, Parkinson J, Rotin D (2007) Ubiquitylation screen using protein microarrays for comprehensive identification of Rsp5 substrates in yeast. *Mol Syst Biol* 3: 116
33. Zhuang M, Guan S, Wang H, Burlingame AL, Wells JA (2013) Substrates of IAP ubiquitin ligases identified with a designed orthogonal E3 ligase, the NEDDylator. *Mol Cell* 49: 273 – 282
34. Mark KG, Simonetta M, Maiolica A, Seller CA, Toczyski DP (2014) Ubiquitin ligase trapping identifies an SCFSaf1 pathway targeting unprocessed vacuolar/lysosomal proteins. *Mol Cell* 53: 148 – 161
35. Yen H-CS, Elledge SJ (2008) Identification of SCF ubiquitin ligase substrates by global protein stability profiling. *Science* 322: 923 – 929
36. Peng J, Schwartz D, Elias JE, Thoreen CC, Cheng D, Marsischky G, Roelofs J, Finley D, Gygi SP (2003) A proteomics approach to understanding protein ubiquitylation. *Nat Biotechnol* 21: 921 – 926
37. Kamadurai HB, Souphron J, Scott DC, Duda DM, Miller DJ, Stringer D, Piper RC, Schulman BA (2009) Insights into ubiquitin transfer cascades from a structure of a UbcH5B-ubiquitin-HECTNEDD4L complex. *Mol Cell* 36: 1095 – 1102

38. Rotin D, Kumar S (2009) Physiological functions of the HECT family of ubiquitin ligases. *Nat Rev Mol Cell Biol* 10: 398 – 409
39. Kaliszewski P, Zoładek T (2008) The role of Rsp5 ubiquitin ligase in regulation of diverse processes in yeast cells. *Acta Biochim Pol* 55: 649 – 662
40. Kim HC, Huibregtse JM (2009) Polyubiquitylation by HECT E3s and the determinants of chain type specificity. *Mol Cell Biol* 29: 3307 – 3318
41. Li E, Pedraza A, Bestagno M, Mancardi S, Sanchez R, Burrone O (1997) Mammalian cell expression of dimeric small immune proteins (SIP). *Protein Eng* 10: 731 – 736
42. Cheung LSL, Kanwar M, Ostermeier M, Konstantopoulos K (2012) A hot-spot motif characterizes the interface between a designed ankyrin-repeat protein and its target ligand. *Biophys J* 102: 407 – 416
43. Wang G, Yang J, Huibregtse JM (1999) Functional domains of the Rsp5 ubiquitin-protein ligase. *Mol Cell Biol* 19: 342 – 352
44. Germann M, Swain E, Bergman L, Nickels JT (2005) Characterizing the sphingolipid signaling pathway that remediates defects associated with loss of the yeast amphiphysin-like orthologs, Rvs161p and Rvs167p. *J Biol Chem* 280: 4270 – 4278
45. Huibregtse JM, Yang JC, Beaudenon SL (1997) The large subunit of RNA polymerase II is a substrate of the Rsp5 ubiquitin-protein ligase. *Proc Natl Acad Sci U S A* 94: 3656 – 3661
46. Andoh T, Hirata Y, Kikuchi A (2002) PY motifs of Rod1 are required for binding to Rsp5 and for drug resistance. *FEBS Lett* 525: 131 – 134
47. Hatakeyama R, Kamiya M, Takahara T, Maeda T (2010) Endocytosis of the aspartic acid/glutamic acid transporter Dip5 is triggered by substrate-dependent recruitment of the Rsp5 ubiquitin ligase via the arrestin-like protein Aly2. *Mol Cell Biol* 30: 5598 – 5607
48. Kee Y, Muñoz W, Lyon N, Huibregtse JM (2006) The deubiquitinating enzyme Ubp2 modulates Rsp5-dependent Lys 63-linked polyubiquitin conjugates in *Saccharomyces cerevisiae*. *J Biol Chem* 281: 36724 – 36731
49. Melino G, Gallagher E, Aqeilan RI, Knight R, Peschiaroli A, Rossi M, Scialpi F, Malatesta M, Zocchi L, Browne G *et al* (2008) Itch: a HECT-type E3 ligase regulating immunity, skin and cancer. *Cell Death Differ* 15: 1103 – 1112
50. Raiborg C, Stenmark H (2009) The ESCRT machinery in endosomal sorting of ubiquitylated membrane proteins. *Nature* 458: 445 – 452
51. Marchese A, Raiborg C, Santini F, Keen JH, Stenmark H, Benovic JL (2003) The E3 ubiquitin ligase AIP4 mediates ubiquitylation and sorting of the G protein-coupled receptor CXCR4. *Dev Cell* 5: 709 – 722
52. Polo S, Sigismund S, Faretta M, Guidi M, Capua MR, Bossi G, Chen H, De Camilli P, Di Fiore PP (2002) A single motif responsible for ubiquitin recognition and monoubiquitylation in endocytic proteins. *Nature* 416: 451 – 455
53. Sette P, Jadwin JA, Dussupt V, Bello NF, Bouamr F (2010) The ESCRT-associated protein Alix recruits the ubiquitin ligase Nedd4-1 to facilitate HIV-1 release through the LYPXnL L domain motif. *J Virol* 84: 8181 – 8192
54. Chen HI, Einbond A, Kwak SJ, Linn H, Koepf E, Peterson S, Kelly JW, Sudol M (1997) Characterization of the WW domain of human Yes-associated protein and its polyproline-containing ligands. *J Biol Chem* 272: 17070 – 17077
55. Ranjitkar P, Press MO, Yi X, Baker R, MacCoss MJ, Biggins S (2010) An E3 ubiquitin ligase prevents ectopic localization of the centromeric histone H3 variant via the centromere targeting domain. *Mol Cell* 40: 455 – 464
56. Hewawasam G, Shivaraju M, Mattingly M, Venkatesh S, Martin-Brown S, Florens L, Workman JL, Gerton JL (2010) Psh1 is an E3 ubiquitin ligase that targets the centromeric histone variant Cse4. *Mol Cell* 40: 444 – 454
57. Deyter GMR, Biggins S (2014) The FACT complex interacts with the E3 ubiquitin ligase Psh1 to prevent ectopic localization of CENP-A. *Genes Dev* 28: 1815 – 1826
58. Rodrigo-Brenni MC, Gutierrez E, Hegde RS (2014) Cytosolic quality control of mislocalized proteins requires RNF126 recruitment to Bag6. *Mol Cell* 55: 227 – 237
59. Mariappan M, Li X, Stefanovic S, Sharma A, Mateja A, Keenan RJ, Hegde RS (2010) A ribosome-associating factor chaperones tail-anchored membrane proteins. *Nature* 466: 1120 – 1124
60. Pinato S, Gatti M, Scandiuzzi C, Confalonieri S, Penengo L (2011) UMI, a novel RNF168 ubiquitin binding domain involved in the DNA damage signaling pathway. *Mol Cell Biol* 31: 118 – 126
61. Doil C, Mailand N, Bekker-Jensen S, Menard P, Larsen DH, Pepperkok R, Ellenberg J, Panier S, Durocher D, Bartek J *et al* (2009) RNF168 binds and amplifies ubiquitin conjugates on damaged chromosomes to allow accumulation of repair proteins. *Cell* 136: 435 – 446
62. Stewart GS, Panier S, Townsend K, Al-Hakim AK, Kolas NK, Miller ES, Nakada S, Ylanko J, Olivarius S, Mendez M *et al* (2009) The RIDDLE syndrome protein mediates a ubiquitin-dependent signaling cascade at sites of DNA damage. *Cell* 136: 420 – 434
63. Devgan SS, Sanal O, Doil C, Nakamura K, Nahas SA, Pettijohn K, Bartek J, Lukas C, Lukas J, Gatti RA (2011) Homozygous deficiency of ubiquitin-ligase ring-finger protein RNF168 mimics the radiosensitivity syndrome of ataxia-telangiectasia. *Cell Death Differ* 18: 1500 – 1506
64. Stewart GS, Stankovic T, Byrd PJ, Wechsler T, Miller ES, Huissoon A, Drayson MT, West SC, Elledge SJ, Taylor AMR (2007) RIDDLE immunodeficiency syndrome is linked to defects in 53BP1-mediated DNA damage signaling. *Proc Natl Acad Sci U S A* 104: 16910 – 16915
65. Mattiroli F, Vissers JHA, Van Dijk WJ, Ikpa P, Citterio E, Vermeulen W, Marteijn JA, Sixma TK (2012) RNF168 ubiquitylates K13-15 on H2A/H2AX to drive DNA damage signaling. *Cell* 150: 1182 – 1195
66. Mattiroli F, Uckelmann M, Sahtoe DD, van Dijk WJ, Sixma TK (2014) The nucleosome acidic patch plays a critical role in RNF168-dependent ubiquitylation of histone H2A. *Nat Commun* 5: 3291
67. Xu Y, Ayrapetov MK, Xu C, Gursoy-Yuzugullu O, Hu Y, Price BD (2012) Histone H2A.Z controls a critical chromatin remodeling step required for DNA double-strand break repair. *Mol Cell* 48: 723 – 733
68. Sarcinella E, Zuzarte PC, Lau PNI, Draker R, Cheung P (2007) Monoubiquitylation of H2A.Z distinguishes its association with euchromatin or facultative heterochromatin. *Mol Cell Biol* 27: 6457 – 6468
69. Leung JW, Agarwal P, Canny MD, Gong F, Robison AD, Finkelstein IJ, Durocher D, Miller KM (2014) Nucleosome acidic patch promotes RNF168- and RING1B/BMI1-dependent H2AX and H2A ubiquitylation and DNA damage signaling. *PLoS Genet* 10: e1004178
70. Lin CH, MacGurn JA, Chu T, Stefan CJ, Emr SD (2008) Arrestin-related ubiquitin-ligase adaptors regulate endocytosis and protein turnover at the cell surface. *Cell* 135: 714 – 725
71. Nikko E, Pelham HRB (2009) Arrestin-mediated endocytosis of yeast plasma membrane transporters. *Traffic* 10: 1856 – 1867
72. Volland C, Urban-Grimal D, Geraud G, Haguenauer-Tsapis R (1994) Endocytosis and degradation of the yeast uracil permease under adverse conditions. *J Biol Chem* 269: 9833 – 9841
73. Blondel M-O, Morvan J, Dupré S, Urban-Grimal D, Haguenauer-Tsapis R, Volland C (2004) Direct sorting of the yeast uracil permease to the endosomal system is controlled by uracil binding and Rsp5p-dependent ubiquitylation. *Mol Biol Cell* 15: 883 – 895

74. Merhi A, Andre B (2012) Internal amino acids promote Gap1 permease ubiquitylation via TORC1/Npr1/14-3-3-dependent control of the Bul arrestin-like adaptors. *Mol Cell Biol* 32: 4510 – 4522
75. Kaliszewski P, Ferreira T, Gajewska B, Szkopinska A, Berges T, Zoładek T (2006) Enhanced levels of Pis1p (phosphatidylinositol synthase) improve the growth of Saccharomyces cerevisiae cells deficient in Rsp5 ubiquitin ligase. *Biochem J* 395: 173 – 181
76. Hesselberth JR, Miller JP, Golob A, Stajich JE, Michaud GA, Fields S (2006) Comparative analysis of *Saccharomyces cerevisiae* WW domains and their interacting proteins. *Genome Biol* 7: R30
77. Wood CS, Hung C-S, Huoh Y-S, Mousley CJ, Stefan CJ, Bankaitis V, Ferguson KM, Burd CG (2012) Local control of phosphatidylinositol 4-phosphate signaling in the Golgi apparatus by Vps74 and Sac1 phosphoinositide phosphatase. *Mol Biol Cell* 23: 2527 – 2536
78. Von Mollard GF, Nothwehr SF, Stevens TH (1997) The yeast V-SNARE Vti1p mediates two vesicle transport pathways through interactions with the t-SNAREs Sed5p and Pep12p. *J Cell Biol* 137: 1511 – 1524
79. Zahedi RP, Sickmann A, Boehm AM, Winkler C, Zufall N, Schönfisch B, Guiard B, Pfanner N, Meisinger C (2006) Proteomic analysis of the yeast mitochondrial outer membrane reveals accumulation of a subclass of preproteins. *Mol Biol Cell* 17: 1436 – 1450
80. Fang D, Elly C, Gao B, Fang N, Altman Y, Joazeiro C, Hunter T, Copeland N, Jenkins N, Liu Y-C (2002) Dysregulation of T lymphocyte function in itchy mice: a role for Itch in TH2 differentiation. *Nat Immunol* 3: 281 – 287
81. Magnifico A, Ettenberg S, Yang C, Mariano J, Tiwari S, Fang S, Lipkowitz S, Weissman AM (2003) WW domain HECT E3s target Cbl RING finger E3s for proteasomal degradation. *J Biol Chem* 278: 43169 – 43177
82. Scharschmidt E, Wegener E, Heissmeyer V, Rao A, Krappmann D (2004) Degradation of Bcl10 induced by T-cell activation negatively regulates NF-kappa B signaling. *Mol Cell Biol* 24: 3860 – 3873
83. Gao M, Labuda T, Xia Y, Gallagher E, Fang D, Liu Y-C, Karin M (2004) Jun turnover is controlled through JNK-dependent phosphorylation of the E3 ligase Itch. *Science* 306: 271 – 275
84. Chen W-T, Alpert A, Leiter C, Gong F, Jackson SP, Miller KM (2012) Systematic identification of functional residues in mammalian histone H2AX. *Mol Cell Biol* 33: 111 – 126
85. McGinty RK, Henrici RC, Tan S (2014) Crystal structure of the PRC1 ubiquitylation module bound to the nucleosome. *Nature* 514: 591 – 596
86. Suto RK, Clarkson MJ, Tremethick DJ, Luger K (2000) Crystal structure of a nucleosome core particle containing the variant histone H2A.Z. *Nat Struct Biol* 7: 1121 – 1124
87. Kee Y, Lyon N, Huibregtse JM (2005) The Rsp5 ubiquitin ligase is coupled to and antagonized by the Ubp2 deubiquitinating enzyme. *EMBO J* 24: 2414 – 2424
88. Kim HC, Steffen AM, Oldham ML, Chen J, Huibregtse JM (2011) Structure and function of a HECT domain ubiquitin-binding site. *EMBO Rep* 12: 334 – 341
89. Tjeertes JV, Miller KM, Jackson SP (2009) Screen for DNA-damage-responsive histone modifications identifies H3K9Ac and H3K56Ac in human cells. *EMBO J* 28: 1878 – 1889
90. Dastur A, Beaudenon S, Kelley M, Krug RM, Huibregtse JM (2006) Herc5, an interferon-induced HECT E3 enzyme, is required for conjugation of ISG15 in human cells. *J Biol Chem* 281: 4334 – 4338
91. Huibregtse JM, Scheffner M, Beaudenon S, Howley PM (1995) A family of proteins structurally and functionally related to the E6-AP ubiquitin-protein ligase. *Proc Natl Acad Sci* 92: 2563 – 2567
92. Gietz RD, Woods RA (2002) Transformation of yeast by lithium acetate/single-stranded carrier DNA/polyethylene glycol method. *Methods Enzymol* 350: 87 – 96
93. Takata K, Reh S, Tomida J, Person MD, Wood RD (2013) Human DNA helicase HELQ participates in DNA interstrand crosslink tolerance with ATR and RAD51 paralogs. *Nat Commun* 4: 2338
94. Fang NN, Chan GT, Zhu M, Comyn SA, Persaud A, Deshaies RJ, Rotin D, Gsponer J, Mayor T (2014) Rsp5/Nedd4 is the main ubiquitin ligase that targets cytosolic misfolded proteins following heat stress. *Nat Cell Biol* 16: 1227 – 1237

Correction added on 2 December 2015 after first online publication: References in the Materials and Methods section were corrected and references [91–93] were added.

